## SYNCHRONOUS MOTOR DRIVES

Synchronous motor drives are used to convert between electrical and mechanical energy in applications which include disk drives in computers, compressors and fans, high-performance servo systems for robotics, and propulsion systems in some electric vehicles. This type of variable-speed drive system offers high efficiency and excellent torque and speed regulation. Figure 1 is a functional representation of a generic synchronous motor drive. A power converter, consisting of a number of power semiconductor switches, converts electrical energy from the power source to a form suitable for supplying the synchronous-machine stator windings. A low-power field exciter supplies the field winding if one is present. The power source is often the electric utility grid, but may also be a battery or another rotating machine. The conversion between electrical and mechanical energy actually takes place in the synchronous machine which may be a wound-rotor machine, a synchronous-reluctance machine, or a permanent-magnet

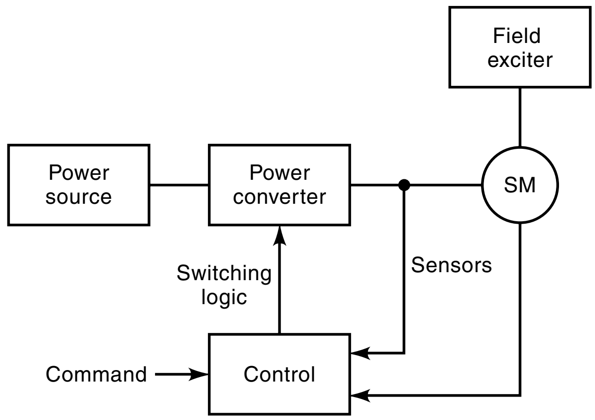


**Figure 1.** Generic synchronous motor drive. The power converter converts energy from the power source (a utility grid, a battery pack, or another machine) to a form suitable for the synchronous machine (SM).

machine. Another important aspect of this system is a sensor array which often includes a rotor positional sensor, current sensors, and voltage sensors. Based on the sensor output and a torque, speed, or other input command, the drive controller determines the on/off status of each of the power converter semiconductors so that the desired performance is achieved.

The operation of synchronous motor drives is dictated by the operating principle of a synchronous machine. Figure 2 is a cross-sectional view of a wound-rotor synchronous machine. The interior of the machine (the rotating member) is called the rotor and the exterior portion (the stationary member) is the stator. Three sets of windings (*as-as′*, *bs-bs′*, and *cs-cs′*) located in the interior of the stator are called phases. Physically, these windings are sinusoidally distributed in slots on the inside of the stator although they are shown in lumped positions in Fig. 2. Three magnetic axes, which are $2\pi/3$ radians apart are associated with each of these three phases. The main rotor winding is the field winding (*fd-fd′*). In addition, the rotor also includes damper 'windings' denoted (*kd-kd′*) and (*kq-kq′*). These windings may not actually be windings at all; instead they often represent currents flowing in aluminum bars in the rotor structure which provide damping torque during electromechanical transients. The $q$ and $d$ axes of the machine denote the magnetic axes of the $q$-axis damper and $d$-axis field and damping windings, respectively. Figure 2 also defines the mechanical rotor position $\theta_{rm}$ of the machine, which is measured from the *as* axis to the $q$ axis. The mechanical rotor speed $\omega_{rm}$ is measured in the counterclockwise direction. For the purpose of machine analysis, it is convenient to define the electrical rotor position $\theta_r$ and the electrical rotor speed, $\omega_r$ as $P/2$ times the corresponding mechanical quantities, where $P$ is the number of poles.

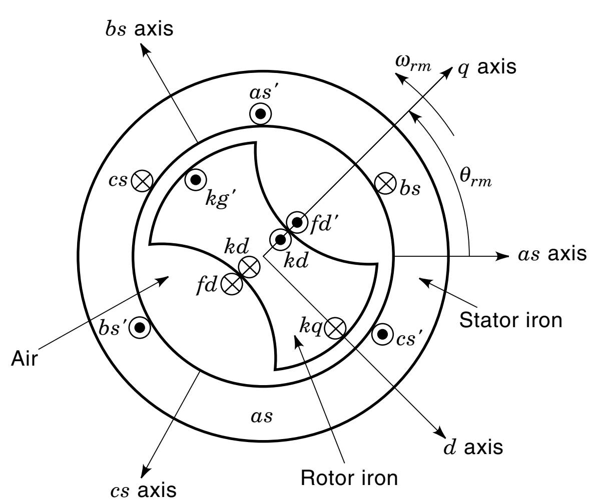


**Figure 2.** Cross-sectional view of a wound-rotor synchronous machine. The stationary member, labeled "stator," contains three sets of windings which are sinusoidally distributed (although they are shown here as lumped coils). The rotating member, labeled "rotor," is a salient structure containing a field winding to produce the rotor MMF and damper windings to produce damping torque during electromechanical transients.

The steady-state operation of a synchronous machine is as follows. First, a dc source is applied to the field winding. This makes the rotor iron in the area where the $d$-axis leaves the rotor a North magnetic pole and the rotor iron on the opposite side a South magnetic pole. Next, a three-phase ac source excites the stator windings. The $a$-, $b$-, and $c$-phase applied voltages have the form

$$v_{as} = \sqrt{2}V_s \cos(\theta_e) \tag{1}$$

$$v_{bs} = \sqrt{2}V_s \cos\left(\theta_e - \frac{2\pi}{3}\right) \tag{2}$$

and

$$v_{cs} = \sqrt{2}V_s \cos\left(\theta_e + \frac{2\pi}{3}\right) \tag{3}$$

where

$$\theta_e = \omega_e t \tag{4}$$

In Eq. (1–4), $V_s$ is the rms amplitude of the applied stator voltage, and $\omega_e$ is the radian frequency. In the steady state, the resulting currents are expressed by

$$i_{as} = \sqrt{2}I_s \cos(\theta_e + \phi_i) \tag{5}$$

$$i_{bs} = \sqrt{2}I_s \cos\left(\theta_e + \phi_i - \frac{2\pi}{3}\right) \tag{6}$$

and

$$i_{cs} = \sqrt{2}I_s \cos\left(\theta_e + \phi_i + \frac{2\pi}{3}\right) \tag{7}$$

where $I_s$ is the rms stator current. Currents of the form Eq. (5–7) result in a rotating magnetomotive force (MMF) which travels counterclockwise around the interior of the stator surface at an angular velocity of $\omega_e$. The interaction of the rotor poles with the stator poles causes the rotor to rotate synchronously with the stator magnetic field. Thus, the electrical rotor speed is $\omega_e$, and the mechanical (physical) rotor speed is $2\omega_e/P$. The fact that the rotor speed is directly tied to the radian frequency of the stator excitation is the defining characteristic of synchronous machines.

To make this observation more quantitative, if the resistance of the stator windings is negligible, the electromagnetic torque produced by a synchronous machine under the stated conditions is given by (1)

$$T_e = -\frac{3}{2}\frac{P}{2}\frac{L_{md}i'_{fd}\sqrt{2}V_s}{\omega_e L_d}\sin\delta - \frac{3}{4}\frac{P}{2}\frac{1}{\omega_e^2}\left(\frac{1}{L_q}-\frac{1}{L_d}\right)(\sqrt{2}V_s)^2\sin 2\delta \tag{8}$$

In Eq. (8), $L_{md}$, $L_d$, and $L_q$ are the $d$-axis magnetizing inductance, the $d$-axis stator self-inductance, and the $q$-axis self-inductance, respectively, $i'_{fd}$ is the referred field current, and $\delta$ is the torque angle of the synchronous machine defined as

$$\delta = \theta_r - \theta_e \tag{9}$$

Physically, the torque angle represents the difference between the electrical rotor position and the instantaneous angle of the applied voltages. In Eq. (8), the first term represents the torque produced by the interaction of the field winding with the stator magnetic field (field torque), and the second term is from the interaction of the rotor iron with the stator magnetic field (reluctance torque). Figure 3 illustrates the field, reluctance, and total torque as a function of torque angle for a 3.7 kW synchronous machine.

Although the wound-rotor synchronous machine just considered is a standard configuration, several important variations are used in electric drive systems. First, from the form of the torque-delta characteristic, specifically the second term in Eq. (8), torque is produced without a field winding. Such machines are known as synchronous-reluctance devices because the torque is produced by reluctance. These machines

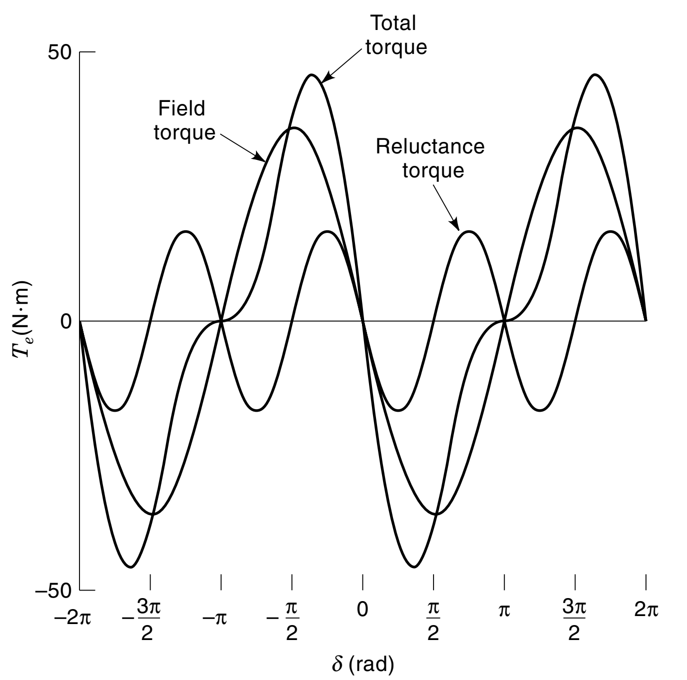


**Figure 3.** Field, reluctance, and total torque as a function of delta. The field torque is produced by the interaction of the stator magnetic field with that of the rotor field winding. The reluctance torque is produced by the interaction of the salient rotor iron and the stator magnetic field.

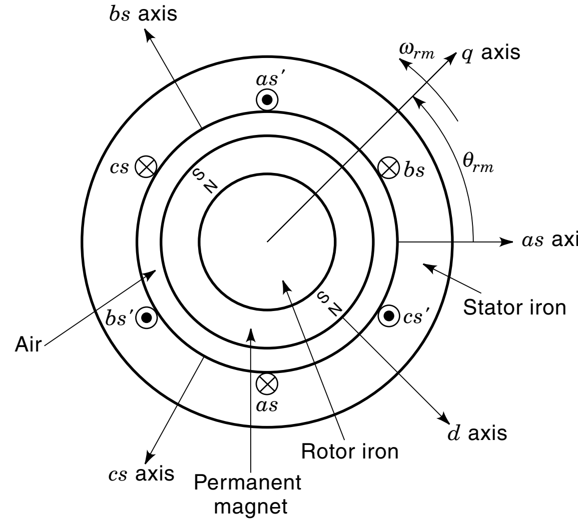


**Figure 4.** Cross-sectional view of a surface-mounted, permanent-magnet, synchronous machine. This machine differs from the configuration in Fig. 2 in that the rotor iron is round and a permanent magnet replaces the wound field.

are less expensive to manufacture than the wound field machines because the field winding and the complication of making electrical connection to the rotating field circuit are eliminated.

In another variation of the synchronous machine, the field winding is replaced with a permanent magnet. There are two variations of this system, the surface-mounted permanent magnet and interior permanent-magnet machines, as depicted in Figs. 4 and 5, respectively. In the surface-mounted case, the magnetic material is mounted on the surface of the rotor. Because of the relatively low permeability of most materials used as permanent magnets, such a machine offers relatively low inductances and thereby good bandwidth for con-

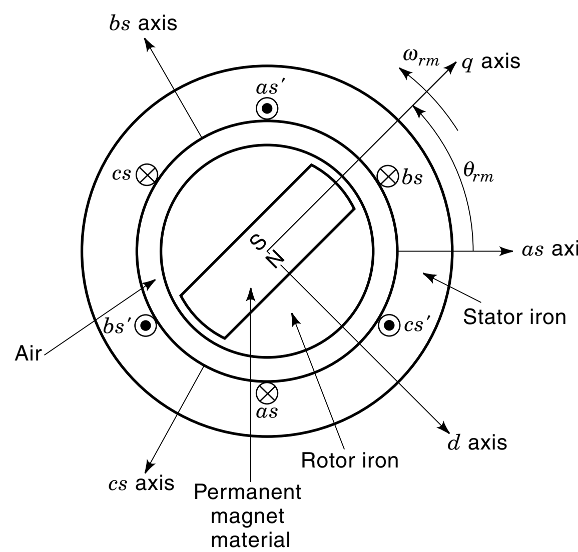


**Figure 5.** Cross-sectional view of a buried, permanent-magnet, synchronous machine. This permanent-magnet machine has magnetic saliency due to the low relative permeability of the magnetic material buried in the rotor iron.

trol applications. Furthermore, such a machine is relatively easy to construct. Although more difficult to construct, the interior or buried permanent-magnet machines are operated at higher speeds than their surface-mounted counterparts because the iron surrounding the mechanically weak permanent magnet adds the structural strength required to withstand high operating speeds.

## MACHINE MODELS

To provide a more quantitative look at synchronous-machine drives, it is first necessary to set forth the mathematical models of the various types of synchronous machines. These models have three parts: the voltage equations which relate the applied voltage to the ohmic voltage drop to winding resistance and the time rate of change of flux linking the various windings; the flux linkage equations which relate the flux linking the individual windings to the current in the windings and electrical rotor position; and finally a torque equation which predicts the electromagnetic torque in terms of the machine current and rotor position. The classical synchronous-machine is based on Park's transformation (2) which is expressed as

$$\begin{bmatrix} f_{qs} \\ f_{ds} \\ f_{0s} \end{bmatrix} = \frac{2}{3} \begin{bmatrix} \cos(\theta_r) & \cos\left(\theta_r - \frac{2\pi}{3}\right) & \cos\left(\theta_r + \frac{2\pi}{3}\right) \\ \sin(\theta_r) & \sin\left(\theta_r - \frac{2\pi}{3}\right) & \sin\left(\theta_r + \frac{2\pi}{3}\right) \\ \frac{1}{2} & \frac{1}{2} & \frac{1}{2} \end{bmatrix} \begin{bmatrix} f_{as} \\ f_{bs} \\ f_{cs} \end{bmatrix} \tag{10}$$

In Eq. (10), $f$ is a stator voltage $v$, stator current $i$, or stator flux linkage $\lambda$. Expressing the machine model in terms of transformed variables results in considerable analytical simplification. In particular, it eliminates rotor-position-dependent inductances from the machine description and also results in a model wherein the various voltages, currents, and flux linkages are constant in the steady state. In addition to expressing the synchronous machine model in terms of transformed stator variables rather than physical variables, it is also convenient to refer the field and damper winding variables to the stator by the appropriate turns ratio. In the case of the field winding, this referral is made by defining the referred field voltage and current as

$$v'_{fd} = \frac{N_s}{N_{fd}} v_{fd} \tag{11}$$

and

$$i'_{fd} = \frac{2}{3}\frac{N_{fd}}{N_s} i_{fd} \tag{12}$$

where $N_s$ and $N_{fd}$ are the effective stator and field turns, respectively. The damper circuits are similarly referred. Because the turns ratio is not needed to use the model and cannot be measured in the laboratory, however, these referred variables are not defined here.

In terms of the transformed and referred variables, the stator and rotor voltage equations are expressed by

$$v_{qs} = r_s i_{qs} + \omega_r \lambda_{ds} + p\lambda_{qs} \tag{13}$$

$$v_{ds} = r_s i_{ds} - \omega_r \lambda_{qs} + p\lambda_{ds} \tag{14}$$

and

$$v_{0s} = r_s i_{0s} + p\lambda_{os} \tag{15}$$

and

$$v'_{kq_i} = r'_{kq_i} i'_{kq_i} + p\lambda'_{kq_i} \quad i \in 1\ldots m \tag{16}$$

$$v'_{fd} = r'_{fd} i'_{fd} + p\lambda'_{fd} \tag{17}$$

and

$$v'_{kd_i} = r'_{kd_i} i'_{kd_i} + p\lambda'_{kd_i} \quad i \in 1\ldots n \tag{18}$$

respectively, where $m$ and $n$ are the number of damper circuits used in the $q$ and $d$ axes and $p$ is heaviside notation for differentiation with respect to time. The stator and rotor flux linkage equations are given by

$$\lambda_{qs} = L_{ls} i_{qs} + \lambda_{mq} \tag{19}$$

$$\lambda_{ds} = L_{ls} i_{ds} + \lambda_{md} \tag{20}$$

and

$$\lambda_{0s} = L_{ls} i_{0s} \tag{21}$$

and

$$\lambda'_{kq_i} = L'_{lkq_i} i'_{kq_i} + \lambda_{mq} \quad i \in 1\ldots m \tag{22}$$

$$\lambda_{fd} = L'_{lfd} i'_{fd} + \lambda_{md} \tag{23}$$

and

$$\lambda'_{kd_i} = L'_{lkd_i} i'_{kd_i} + \lambda_{md} \quad i \in 1\ldots n \tag{24}$$

In Eqs. (19–24), $\lambda_{mq}$ and $\lambda_{md}$ are the $q$- and $d$-axis magnetizing flux linkages defined as

$$\lambda_{mq} = L_{mq}\left(i_{qs} + \sum_{i=1}^{m} i_{kq_i}\right) \tag{25}$$

and

$$\lambda_{md} = L_{md}\left(i_{ds} + \sum_{i=1}^{n} i_{kd_i} + i'_{fd}\right) \tag{26}$$

Finally, electromagnetic torque, in terms of the transformed variables, is expressed as

$$T_e = \frac{3}{2}\frac{P}{2}(\lambda_{ds} i_{qs} - \lambda_{qs} i_{ds}) \tag{27}$$

Figure 6 illustrates an equivalent circuit consistent with Eqs. (13–26). It is worth noting that the model is valid for

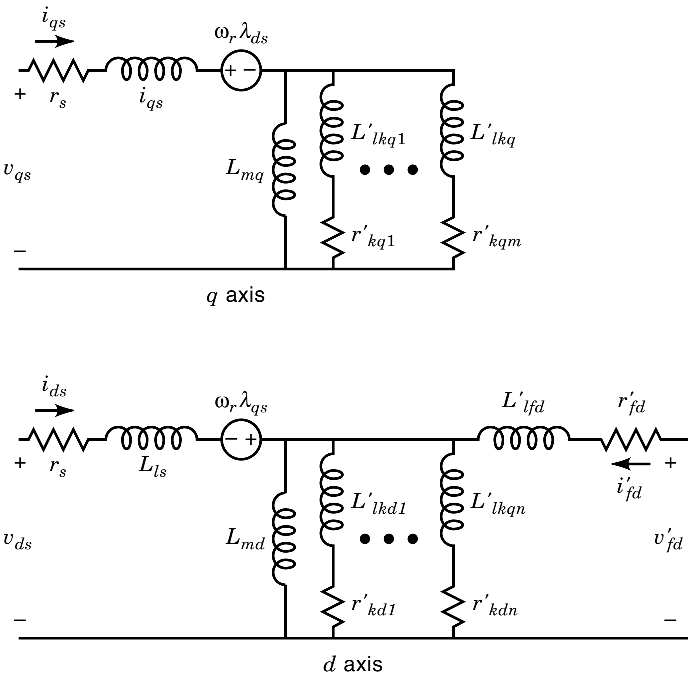


**Figure 6.** Synchronous-machine equivalent circuit based on Park's transformation.

transient and steady-state conditions. At the same time, however, the reader is cautioned that the model has been set forth in a simple form. Important secondary effects, such as magnetic saturation of the magnetizing path, are not included, but are discussed in (3,4,5). For a detailed discussion of the derivation of the model, the reader is referred to (1).

Before concluding this section, it is appropriate to consider briefly the models of the synchronous-reluctance and the permanent-magnet machines. In the case of the reluctance machine, the model is identical to that of the wound-rotor synchronous machine except that the field current is set to zero and the field voltage equation is eliminated from the machine description. In the case of the permanent-magnet machines, the machine model is obtained by (1) eliminating all damper currents and voltage equations from the machine description (because the rotor currents in this type of machine are normally negligible) and (2) treating the field current as a constant. After making these changes and combining the flux linkage equations with the voltage equations,

$$v_{qs} = r_s i_{qs} + \omega_r L_d i_{ds} + L_q p i_{qs} + \omega_r \lambda_m \tag{28}$$

$$v_{ds} = r_s i_{ds} - \omega_r L_q i_{qs} + L_d p i_{ds} \tag{29}$$

and

$$v_{0s} = r_s i_{0s} + L_{ls} p i_{0s} \tag{30}$$

In Eqs. (28–30), $L_q$ and $L_d$ are the stator $q$- and $d$-axis self-inductances and $\lambda_m$ is a constant related to the strength of the permanent magnet (the fictitious, constant, field current), the number of stator winding turns per phase, and the machine geometry. The torque equation becomes

$$T_e = \frac{3}{2}\frac{P}{2}[\lambda_m i_{qs} + (L_d - L_q) i_{qs} i_{ds}] \tag{31}$$

As in the case of the wound-rotor machine, this model is valid for both steady-state and transient conditions. The model is also valid for both surface-mounted and interior-mounted, permanent-magnet machines, although, in the case of surface-mounted machines, $L_q$ and $L_d$ equal. Therefore, both of these symbols are normally replaced by the symbol $L_{ss}$ when working with surface-mounted, permanent-magnetic machines. It is also worth noting that, unlike a wound-rotor synchronous machine in which $L_d > L_q$, in the case of the interior permanent-magnet machine, $L_q > L_d$ because the permanent magnetic increases the reluctance of the $d$-axis magnetic path. For most applications, the model in Eqs. (28–31) is quite accurate. The reader should be aware, however, that it is only valid in machines with sinusoidal back-emfs. For analysis of machines with nonsinusoidal back-emfs, the reader is referred to (6,7).

## POWER CONVERTERS

The most important component of a synchronous machine drive system is the power converter, which takes numerous forms depending on whether the input is ac or dc. In most applications, the input power is directly obtained from a dc source or else a dc source is constructed by rectifying the ac input to the drive. Therefore, it is appropriate to focus on converting electrical energy from dc to ac, which is accomplished by a device called an inverter. The most prevalent topology for an inverter designed for a three-phase machine is the three-phase, fully controlled, bridge converter depicted in Fig. 7, showing the converter connected to a machine in a wye configuration. In this device, each of the transistors is a variety of fully controlled semiconductor devices (that is, they are turned on and turned off at times specified by the gating signals T1–T6) including bipolar junction transistors (BJT), metal oxide semiconductor field effect transistors (MOSFET), insulated gate bipolar transistors (IGBT), MOS controlled thyristors (MCT). Regardless of the technology used to manu-

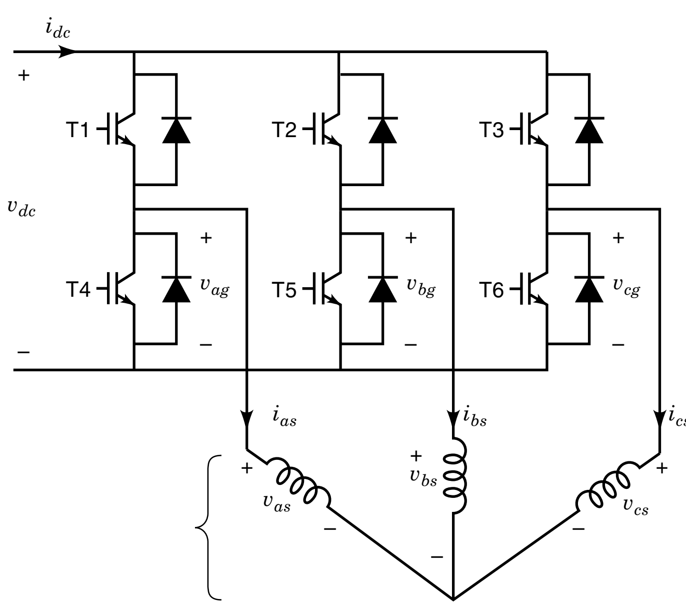


**Figure 7.** Fully controlled, three-phase bridge inverter and wye-connected load.

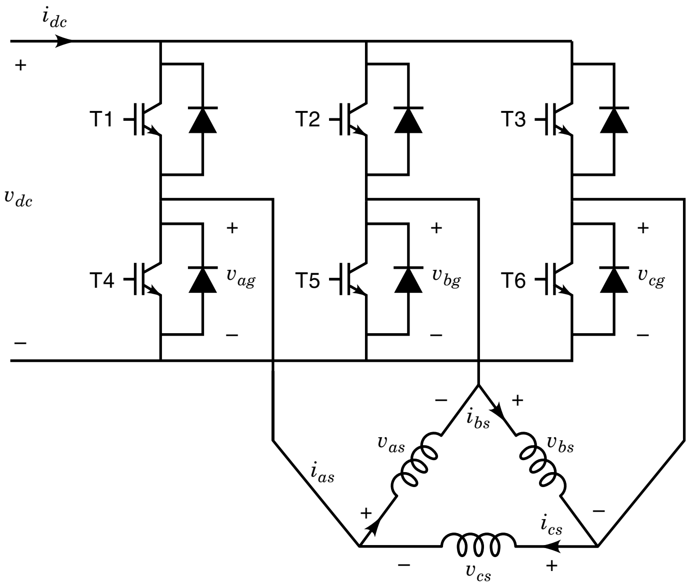


**Figure 8.** Fully controlled, three-phase bridge inverter with delta-connected load.

facture the transistors, they are always operated in the saturated or the cutoff region of their $i$–$v$ characteristic, that is, completely on or completely off. Under these conditions, the voltage across or current through the semiconductor device is always zero which prevents excessive power dissipation within the semiconductors.

To analyze the three-phase, fully controlled, bridge converter feeding a wye-connected load, it is convenient to note that, for any of the machines considered in the previous section, the sum of the line-to-neutral voltages must be zero. Using this property,

$$v_{as} = \frac{2}{3}v_{ag} - \frac{1}{3}v_{bg} - \frac{1}{3}v_{cg} \tag{32}$$

$$v_{bg} = -\frac{1}{3}v_{ag} + \frac{2}{3}v_{bg} - \frac{1}{3}v_{cg} \tag{33}$$

and

$$v_{cg} = -\frac{1}{3}v_{ag} - \frac{1}{3}v_{bg} + \frac{2}{3}v_{cg} \tag{34}$$

In the case of a delta-connected machine, illustrated in Fig. 8,

$$v_{as} = v_{ag} - v_{bg} \tag{35}$$

$$v_{bs} = v_{bg} - v_{cg} \tag{36}$$

and

$$v_{cs} = v_{cg} - v_{ag} \tag{37}$$

Using Eqs. (32–34) or Eqs. (35–37), the voltages applied to the machine are readily established in terms of the line-to-ground voltages. Neglecting the forward diode and transistor voltage drops, these voltages are expressed by

$$v_{ag} = \begin{cases} v_{dc} & \text{T1 on, T4 off} \\ 0 & \text{T1 off, T4 on} \end{cases} \tag{38}$$

$$v_{bg} = \begin{cases} v_{dc} & \text{T2 on, T5 off} \\ 0 & \text{T2 off, T5 on} \end{cases} \tag{39}$$

and

$$v_{ag} = \begin{cases} v_{dc} & \text{T3 on, T6 off} \\ 0 & \text{T3 off, T6 on} \end{cases} \tag{40}$$

In Eqs. (38–40), it is assumed that one, and only one, active semiconductor of each phase leg is conducting. Operation with two devices simultaneously conducting is normally not allowed because this would short circuit the dc source. Operation with neither device on is occasional. However, analyzing this condition is quite involved and so the reader is referred to (8,9,10).

At this point, we have set forth the relationships necessary to predict the voltages applied to the machine, given the dc voltage and on/off status of the semiconductor switches. It is now possible to use these relationships to explain the inverter operation. There are two principal modes of operating the fully controlled, three-phase bridge whereby it can be used to convert power from dc to ac. These modes are voltage-source inverter (VSI) operation and current-regulated inverter (CRI) operation. The most basic method of converting power from dc to ac is to switch the transistors, as illustrated in Fig. 9, where a wye-connected load is considered. Using the stated gating signals and the relationships in Eqs. (32–34), one obtains the line-to-neutral voltage depicted in the figure. Because this mode of operation consists of a repetition of six switching states, it is called a six-step operation. It is also commonly called a 180° voltage-source inverter (180° VSI) operation. The resulting line-to-neutral voltages, although ac, possess considerable harmonic content which results in increased machine losses. Nevertheless, this strategy is often used for permanent-magnet synchronous motor drives because it is one of the least expensive strategies. For the purposes of analysis, machines operated from the three-phase bridge by this control strategy respond primarily to the fundamental component of the applied voltages except at very low speeds (frequencies). The fundamental component of the applied voltages is expressed as

$$v_{as,fund} = \frac{2}{\pi}v_{dc}\cos(\theta_c) \tag{41}$$

$$v_{bs,fund} = \frac{2}{\pi}v_{dc}\cos\left(\theta_c - \frac{2\pi}{3}\right) \tag{42}$$

and

$$v_{cs,fund} = \frac{2}{\pi}v_{dc}\cos\left(\theta_c + \frac{2\pi}{3}\right) \tag{43}$$

where $\theta_c$ is an independent variable which is related to the rotor position for closed-loop switching controls, as described in later sections. In the event that the machine is delta-con-

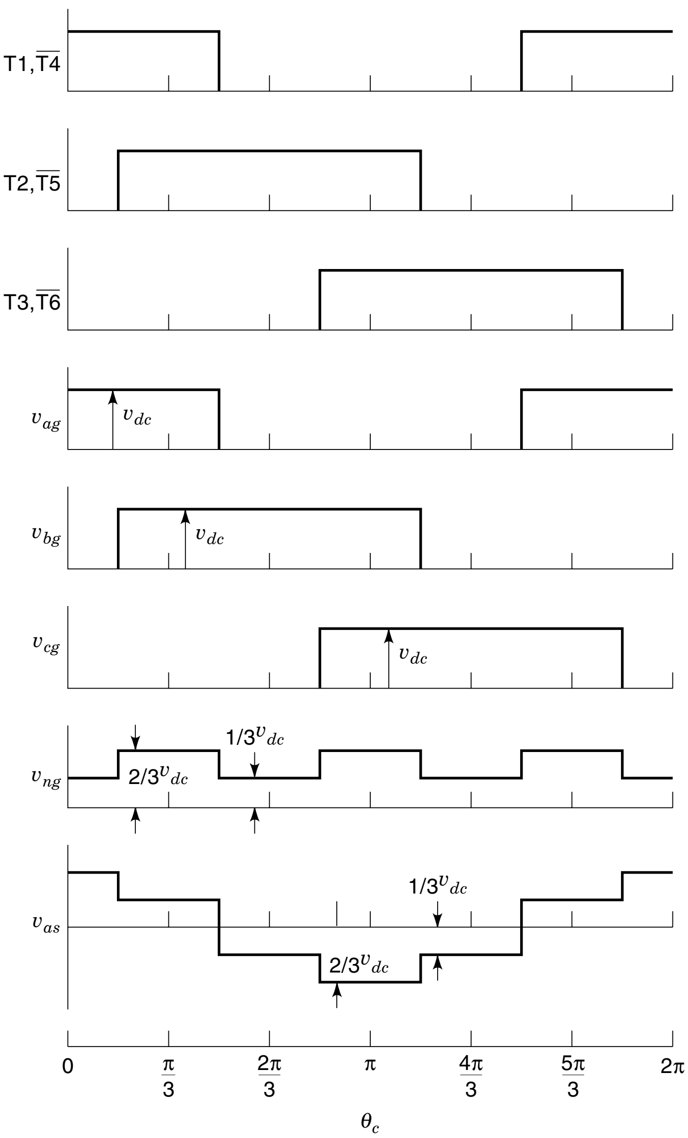


**Figure 9.** Gating signals and inverter voltages for 180° voltage source operation. The $b$- and $c$-phase voltages are identical to the $a$-phase voltage $v_{as}$ with phase lags of $2\pi/3$ and $-2\pi/3$, respectively.

nected Eqs. (41–43) are adjusted by multiplying the amplitude by $\sqrt{3}$ and adding $\pi/6$ to each of the cosine terms.

The next level of sophistication in the control of the fully controlled bridge converter is applying duty-cycle modulation to the switching signals, as illustrated in Figure 10. There, the signals S1, S2, and S3 are identical to T1, T2, and T3 in the case of a six-step operation. The commanded duty cycle $d$ is compared to a high-frequency triangular wave $tr$, which varies between zero and one. If the duty cycle is greater than the triangular wave, the resulting line-to-neutral voltages are the same as in a six-step operation. Otherwise, they are zero. The net effect is that the fundamental components of the applied voltages become

$$v_{as,fund} = \frac{2}{\pi} v_{dc} d \cos(\theta_c) \tag{44}$$

$$v_{bs,fund} = \frac{2}{\pi} v_{dc} d \cos\left(\theta_c - \frac{2\pi}{3}\right) \tag{45}$$

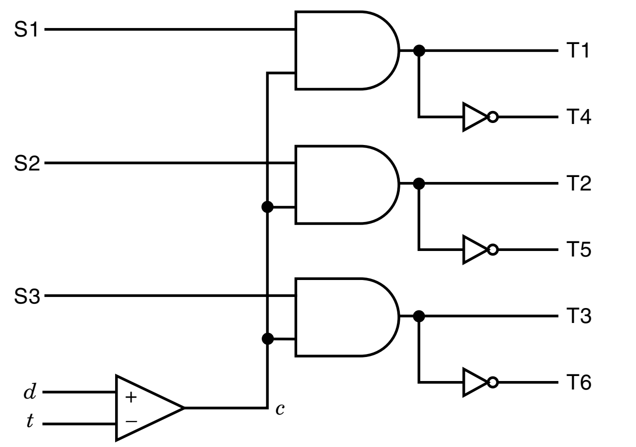


**Figure 10.** Duty-cycle modulating, switch-control algorithm. The net effect of the duty-cycle control is to directly control the amplitude of the machine phase voltages from the control signal $d$.

and

$$v_{cs,fund} = \frac{2}{\pi} v_{dc} d \cos\left(\theta_c + \frac{2\pi}{3}\right) \tag{46}$$

The advantage of this control is that the amplitudes of the applied voltages are readily controlled. The low-frequency voltage harmonics are present just as in the case of a six-step operation. In addition, the high-frequency harmonic content increases but is less important because of the filtering action of the machine inductance. When the machine is delta-connected rather than wye-connected, the changes to the fundamental components of the applied voltage are the same as those made in the case of a six-step operation.

The primary disadvantage of a six-step operation and duty-cycle modulation is the low-frequency harmonic content. There are several strategies for controlling the fully controlled, bridge converter in which low-frequency harmonics are completely eliminated. A diagram illustrating one of these strategies, sine-triangular modulation, is illustrated in Figure 11. There, instantaneous duty cycles for each of the three

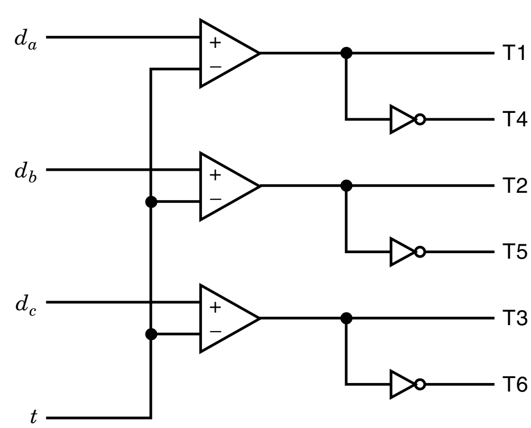


**Figure 11.** Sine-triangle modulating switch-control algorithm. The fundamental component of the resulting $a$- $b$- and $c$-phase line-to-neutral voltages using this control strategy are in phase with and proportional to the magnitudes of the instantaneous phase duty cycles $d_a$, $d_b$, and $d_c$ provided that the signals constitute a balanced set.

phases denoted $d_a$, $d_b$, and $d_c$ are compared to a high frequency triangular wave which varies between $-1$ and 1. The result of this comparison yields the gating signal to each of the inverter semiconductors. Assuming that the instantaneous duty cycles sum to zero and that the absolute value of each of the duty cycles is less than 1, neglecting high-frequency harmonics,

$$v_{as,fund} = \frac{1}{2} d_a v_{dc} \tag{47}$$

$$v_{bs,fund} = \frac{1}{2} d_b v_{dc} \tag{48}$$

and

$$v_{cs,fund} = \frac{1}{2} d_c v_{dc} \tag{49}$$

By commanding the duty cycles as

$$d_a = d\cos(\theta_c) \tag{50}$$

$$d_b = d\cos\left(\theta_c - \frac{2\pi}{3}\right) \tag{51}$$

$$d_c = d\cos\left(\theta_c + \frac{2\pi}{3}\right) \tag{52}$$

where $d$ is the duty cycle (which is a constant as long as the amplitudes of the applied voltages are constant) the line-to-neutral voltages become

$$v_{as,fund} = \frac{1}{2} d v_{dc} \cos(\theta_c) \tag{53}$$

$$v_{bs,fund} = \frac{1}{2} d v_{dc} \cos\left(\theta_c - \frac{2\pi}{3}\right) \tag{54}$$

and

$$v_{cs,fund} = \frac{1}{2} d v_{dc} \cos\left(\theta_c + \frac{2\pi}{3}\right) \tag{55}$$

As with duty-cycle modulation, the amplitude of the applied voltages is readily controlled. However, at the same time, there are important differences. First, low-frequency harmonics are avoided. There is a price paid for eliminating these harmonics. The maximum amplitude of the fundamental component of the line-to-neutral phase voltages which is achieved is now limited to $(1/2)v_{dc}$. Although it is possible to increase the amplitude further, such action introduces low-frequency harmonics. For this reason, other techniques, such as space vector modulation (11), have been developed which also avoid low-frequency harmonics but offer a greater maximum amplitude compared with sine-triangle modulation.

An example of a current regulated inverter control algorithm is hysteresis current control. This strategy assumes the existence of a current command signal for each phase. Then the inverter semiconductors are switched so that the actual currents are always within a prespecified bound (the hysteresis level) of the commanded current. Figure 12 illustrates the switching-state transitional diagram for the $a$-phase of the inverter where the commanded $a$-phase current is denoted $i_{as}^*$. Whenever the actual current exceeds the commanded current by the hysteresis level $h$, the lower transistor of the leg (T4) is turned on, and the upper transistor (T1) is turned off, so that the current decreases. Conversely, if the actual current falls below the commanded current by an amount $h$, the lower transistor (T4) is turned off, and the upper transistor (T1) is turned on, which increases the current. For delta-connected machines, $i_{as}^*$ and $i_{as}$ are replaced by $(i_{as}^* - i_{cs}^*)$ and $(i_{as} - i_{cs})$, respectively, in the hysteresis control. The $b$- and $c$-phases are controlled similarly. The net result of this switching is that, ideally, the actual current is always within $h$ of the commanded current. There are restrictions to this, however. First, a step change in current command necessarily causes the actual current to deviate from the commanded current by an amount exceeding the hysteresis level because the actual current does not change instantaneously under an inductive or motor load. Furthermore, even for steady-state conditions, if the actual currents are within $h$ of the commanded currents, the rms value of the fundamental component of the motor phase voltages must satisfy

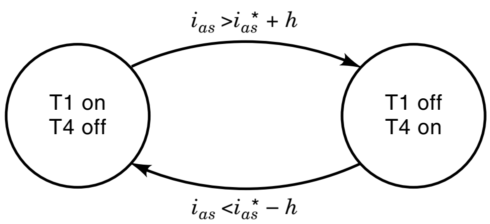


**Figure 12.** Hysteresis current-regulated, switch-control algorithm. Using this algorithm, the converter switching is based on comparing the error between the commanded currents and the actual currents to a threshold level $h$.

$$v_s < \frac{1}{\sqrt{6}} v_{dc} \tag{56}$$

if the machine is wye-connected or

$$v_s < \frac{1}{\sqrt{2}} v_{dc} \tag{57}$$

if the machine is delta-connected. If this constraint is not satisfied, the actual current deviates significantly from the commanded current, a condition called a loss of current tracking.

Although fully controlled, three-phase bridge converters are the dominant technology for constructing inverters, other technologies are used in industrial applications. Figure 13 depicts a three-phase, semicontrolled bridge converter connected to a voltage-behind-reactance ac source. The most important difference between the semicontrolled, three-phase bridge and its fully controlled counterpart is that semicontrolled semiconductors, and, in particular, thyristors, are used rather than fully controllable semiconductors. Thyristor devices are considered semicontrollable because, although they are gated on at any time, they actually turn on only if forward biased and cannot be actively turned off. Turn off occurs whenever the current through the device attempts to become negative. Although this makes the control of the converter less straightforward and eliminates most of the modulation strategies available in the fully controlled case, this type of converter has the advantage that the maximum volt-

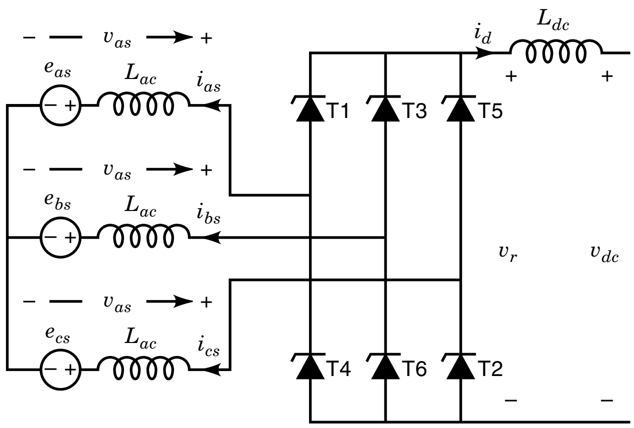


**Figure 13.** Semicontrolled, three-phase bridge converter. This converter contains semicontrolled semiconductors with high voltage and current ratings appropriate for high-power applications.

age and current ratings available in thyristor devices exceed those available in fully controlled semiconductors. For this reason, semicontrolled, three-phase, bridge converters are most often used in high-power synchronous motor drives.

Semicontrolled bridge converters are used either as controlled rectifiers, or as inverters. Figure 14 illustrates the operation of the three-phase bridge converter in rectifier mode with the dc current $i_d$ constant. The upper trace illustrates the three-phase sinusoidal voltage source which represents the back-emf of the machine. The point at which the various thyristors are turned on is indicated directly underneath this trace. The control of this converter is tied to the amount of delay from the time the line-to-neutral voltages cross each other to the point at which the individual thyristors are fired. For example, valve three is fired at a firing angle $\alpha$ after $e_{bs}$ becomes greater than $e_{as}$, or, more formally, when

$$\theta_c = \alpha + \frac{\pi}{3} \tag{58}$$

Assuming the firing pattern shown and that the dc current is constant, the resulting ac currents are illustrated in the next three traces of Fig. 14. It is interesting to observe that, each time a new thyristor is turned on, it causes the current in the thyristor, which was turned on $2\pi/3$ radians previously, to pass through zero whereupon it turns off. This process is called commutation, and the angle between the point where one device begins to conduct and the device gated on $2\pi/3$ radians previously ceases to conduct is called the commutation angle $u$. For overly large dc currents or firing delays, it is possible that commutation does not occur (a commutation failure) which prevents the converter from operating satisfactorily. The final trace illustrates the rectified output voltage. The most pronounced feature in the figure is the notch which occurs during the commutation process.

Analyzing the semicontrolled, three-phase, bridge converter is normally quite involved, because a synchronous machine cannot be modeled accurately in a voltage-behind-inductance form (unless the subtransient inductances are equal, but this is actually never the case). However, neglecting commutation, the average rectifier voltage is given by

$$\overline{v}_d = \frac{3\sqrt{3}}{\pi}\sqrt{2}E\cos\alpha \tag{59}$$

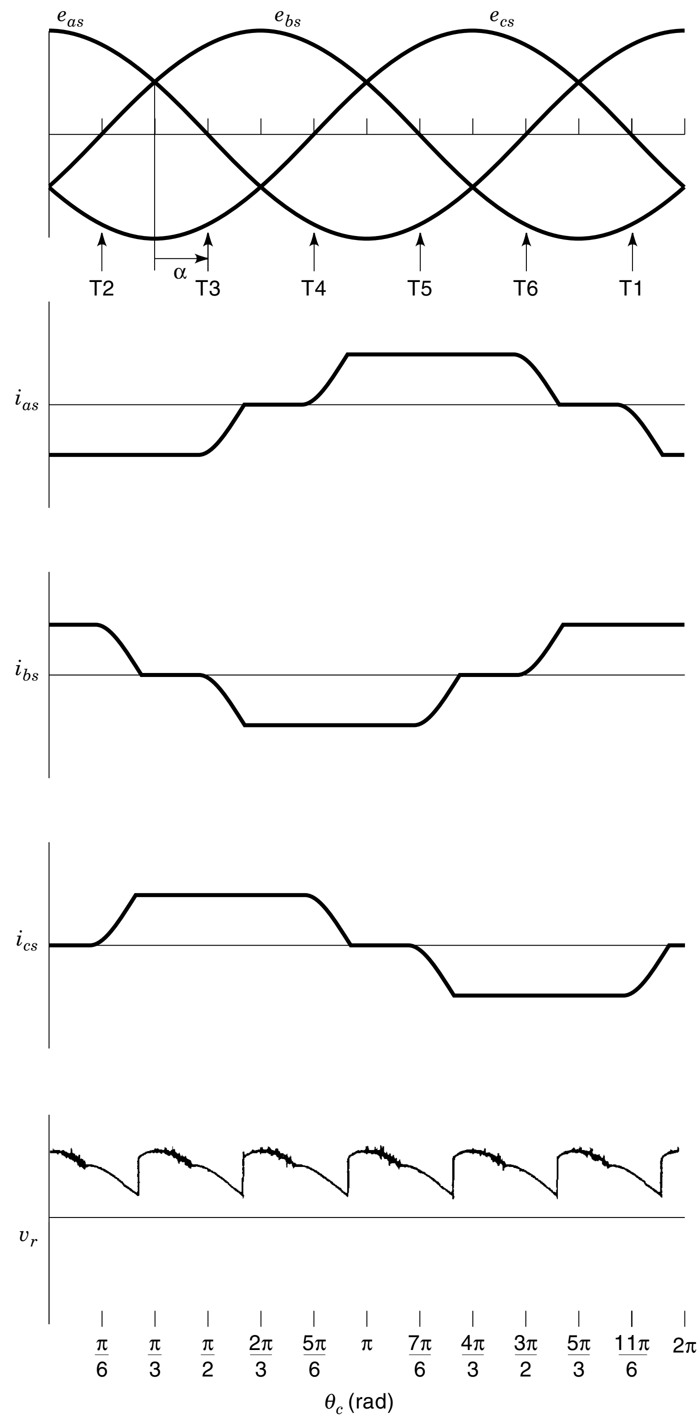


**Figure 14.** Operation of a three-phase semicontrolled converter in rectifier mode. The three-phase voltages represent the machine's back-emf. The arrows beneath these voltages indicate the rotor position at which the various thyristors are turned on. The phase currents are the result of the firing sequence assuming that the dc current is constant. The notch in the rectifier voltage results from the phase current commutation.

and the fundamental components of the ac current are given by

$$i_{as} = \frac{2\sqrt{3}}{\pi} i_d \cos(\theta_c - \alpha + \pi) \tag{60}$$

$$i_{bs} = \frac{2\sqrt{3}}{\pi} i_d \cos\left(\theta_c - \alpha + \pi - \frac{2\pi}{3}\right) \tag{61}$$

and

$$i_{cs} = \frac{2\sqrt{3}}{\pi} i_d \cos\left(\theta_c - \alpha + \pi + \frac{2\pi}{3}\right) \tag{62}$$

From Eq. (59), for firing angles between 0 and $\pi$ radians, the average rectifier voltage is positive. Because the dc current must be positive, power must be flowing out of the machine, and so the converter acts as a rectifier. However, as the firing delay is increased past $\pi$ radians, the average rectifier voltage is negative, and so power flows from the dc side of the converter to the ac side. Therefore, for firing angles greater than $\pi$ radians, the converter operates as an inverter. It may appear that the optimal phase delay is $2\pi$ radians, which maximizes power transfer as an inverter, and in practice the firing delay angle is maximized for inverter operation. The possibility of commutation failure, however, limits the maximum phase delay achievable in this type of converter (12).

## GENERAL CONTROL PHILOSOPHY

Regardless of whether the machine is excited from a fully controlled or semicontrolled inverter, the synchronous machine always operates at a speed corresponding to the frequency of the applied voltage and current providing a very easy means of speed control. In particular, by simply operating the inverter at a frequency corresponding to the desired speed, the torque angle automatically adjusts itself so that the electromagnetic torque is equal to the load torque, subject to the conditions that (1) the load torque is greater than the minimum and less than the maximum electromagnetic torque produced in accordance with the torque versus torque angle characteristic, (2) the system is dynamically stable for the given load torque, and (3) the rate at which the frequency is varied and the way the load torque varies with speed are such that transient stability is maintained during startup. Because the torque angle automatically adjusts itself to the correct value to satisfy the load torque and because the speed must match the applied frequency, this open-loop type of speed control is attractive in that no rotor position or speed sensors are required. In practice, however, conditions (2) and (3) limit the use of this type of control. The alternative is closed-loop control in which rotor position $\theta_r$ is measured and $\theta_c$ is calculated by

$$\theta_c = \theta_r + \phi_v \tag{63}$$

The added phase shift $\phi_v$ is calculated on the basis of a desired torque angle (in fact, $\phi_v = -\delta$; the difference in nomenclature is that $\phi_v$ is traditionally used by drive engineers, whereas $\delta$ is used by power system engineers). In this arrangement, the speed varies until the load torque is satisfied, and the regulation of the speed requires an additional speed control loop. This latter approach typically mitigates stability issues at the cost of additional sensors and control complexity.

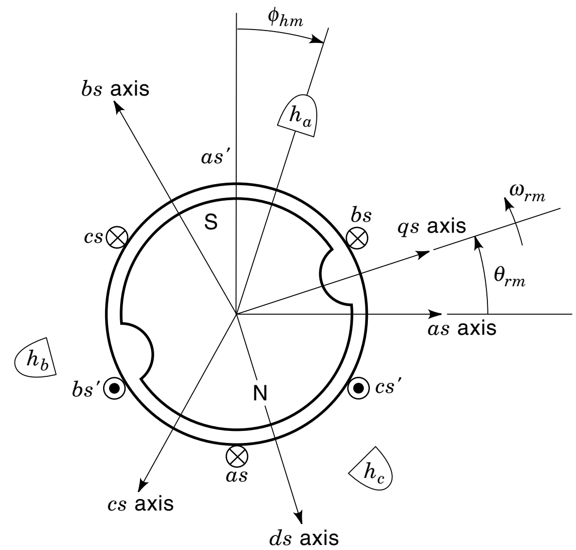


**Figure 15.** Hall-effect sensors mounted on a permanent-magnet synchronous machine. In a practical machine, the sensors are mounded close to the permanent magnet on the end cap or buried in the stator iron. The main purpose of this figure is to show the position of the sensors and the phase shift $\phi_{hm}$.

## SENSOR REQUIREMENTS

The closed-loop control of synchronous motor drives requires a rotor position sensor to $\theta_r$. For the 180° VSI switching strategy, rotor position is determined by inexpensive Hall-effect sensors mounted on the stator as shown in Fig. 15 where $\phi_{hm}$ denotes the angle of mechanical shift of the sensors from the reference position shown. These sensors put out a logic high when under a South magnetic pole and a logic how when under a North magnetic pole to produce the logic signals as a function of rotor position as shown in Fig. 16 where the electrical phase shift angle $\phi_h$ is related to the mechanical phase shift by the number of pole pairs or $\phi_h = (P/2)\phi_{hm}$. Note that

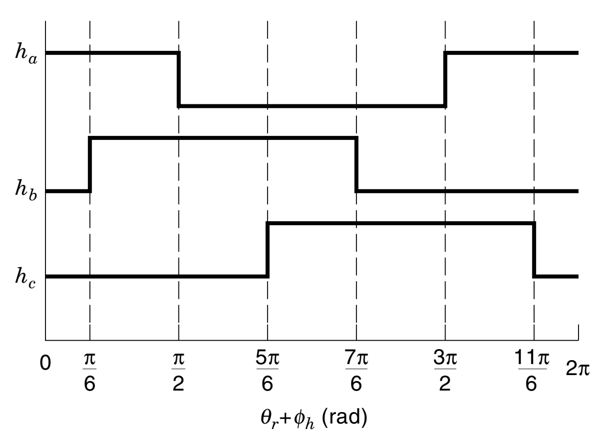


**Figure 16.** Hall-effect logic signals. These signals are identical to the control signals required for 180° VSI operation and thus provide a convenient and inexpensive implementation of that control.

the signals produced by the Hall-effect sensors are identical to the signals of the 180° VSI control shown in Fig. 9 with $\phi_v = \phi_h$. In most 180° VSI drives, the control signals generated directly from the Hall-effect sensor signals provide a convenient and inexpensive implementation.

For high-performance switching strategies, such as sine-triangular modulation or hysteresis current control, in which the commanded voltage or current is a sinusoidal function of rotor position, the rotor position must be measured continuously. This high-resolution measurement usually requires an optical encoder (13) or a resolver (14) which adds expense to the drive. Although the encoder or resolver can be eliminated by using a full observer to determine rotor position, these methods usually require an elaborate scheme for start-up (15,16), and cannot guarantee a bound on the initial error. Furthermore, these methods generally require knowledge of the motor parameters. Recently a hybrid observer was developed which senses rotor position continuously with inexpensive Hall-effect sensors (17). This observer does not require knowledge of motor parameters or an elaborate start-up scheme. Furthermore, the error in estimating the rotor position is bounded by a limit which is independent of operating conditions. Besides rotor position, some synchronous-machine drive controls require motor current or voltage measurements to operate. For example, hysteresis current control requires measuring the stator currents. Closed-loop, Hall-effect sensors, which produce electrically isolated current measurement, are often used for this purpose.

## GENERAL RELATIONSHIPS FOR ANALYZING DRIVE SYSTEMS

Before setting forth a quantitative analysis of synchronous-machine drives, it is appropriate to set forth some concepts and relationships which hold regardless of the type of drive considered. The first concept is that of average-value modeling. In a synchronous machine, in which a balanced three-phase set of voltages is applied, the resulting $q$- and $d$-axis voltages and currents are constant. However, in a drive system, switching of the semiconductors results in $q$- and $d$-axis voltages and currents which are nonconstant. For many purposes, it is sufficient to treat the machine as if the $q$- and $d$-axis quantities were constants equal to their average values. In terms of ac variables, this is equivalent to representing only the fundamental component. In the remainder of this article, average-value quantities are designated with an overbar. Another useful concept is that $q$- and $d$-axis quantities are readily related to the phasor representation of the ac variables. In particular, the rms amplitude $f_s$ and phase $\phi_s$ (relative to rotor position) of a phasor representation of the fundamental component of stator quantity is related to the $q$- and $d$-axis components by

$$f_s = \frac{1}{\sqrt{2}}\sqrt{\overline{f}_{qs}^2 + \overline{f}_{ds}^2} \tag{64}$$

$$\phi_s = \text{angle}(\overline{f}_{qs} - j\overline{f}_{ds}) \tag{65}$$

where $f$ is a stator voltage, current, or flux linkage. The power into a synchronous machine is expressed in terms of $q$- and $d$-variables as

$$\overline{P}_{\text{in}} = \frac{3}{2}(\overline{v}_{qs}^r \overline{i}_{qs}^r + \overline{v}_{ds}^r \overline{i}_{ds}^r) \tag{66}$$

and average output power is given by

$$\overline{P}_{\text{out}} = \overline{T}_e \omega_{rm} \tag{67}$$

In Eq. (66) the power calculation is an approximation because the average of the product of two terms (the voltage and current) is replaced by the product of the averages. This approximation works well in practice (18). Machine efficiency is calculated by

$$\text{eff} = \frac{\overline{P}_{\text{out}}}{\overline{P}_{\text{in}}} \tag{68}$$

If the power electronic converter losses are neglected, another useful relationship applicable to any drive system is that the average dc current is found from the input power by

$$\overline{i}_{dc} = \frac{\overline{P}_{\text{in}}}{v_{dc}} \tag{69}$$

For this discussion, it is assumed that the dc voltage is constant.

With these basic relationships now in place, the performance of a variety of synchronous motor drives is investigated in detail. First, voltage and current source operation of permanent-magnet, synchronous machine drives are addressed. These drives are used widely in industry and are replacing standard brush-type dc motors in many applications. Because their performance is similar to dc motors, they are often times called brushless dc motors. The next configurations considered are voltage and current source operation of reluctance motor drives. Because synchronous-reluctance motors are usually driven from the 60 Hz line in open-loop mode to obtain constant speed, this configuration is not as widely used and so is only discussed briefly. Finally, wound-rotor synchronous motor drive using semicontrolled bridge converters are considered.

## VOLTAGE-SOURCE, INVERTER-FED, PERMANENT-MAGNETIC, SYNCHRONOUS MACHINE DRIVES

One of the most common synchronous motor drive configurations is based on a three-phase, fully controlled, inverter feeding a permanent-magnet synchronous machine. This arrangement is always operated in a closed-loop with respect to rotor position. The operation of such a drive is illustrated in Figure 17, which depicts the performance of a 560 W brushless dc motor drive whose parameters are listed in Table 1. In this system, Hall-effect sensors generate gate signals to the inverter which is operated in the six-step mode. The sensors are arranged so that the phase advance is zero. In the study, the dc voltage is 267 V and the mechanical speed is 314.2 rad/s. Variables depicted include the motor $a$-phase voltage $v_{as}$, $a$-phase current $i_{as}$, and torque $T_e$ predicted by a computer simulation. As can be seen, the $a$-phase voltage waveform is a stepped approximation to a cosine waveform. The resulting machine currents contain low-frequency harmonics which produce low-frequency torque ripple. This is eliminated by sine-triangle modulation (note that continuous rotor position sensing is required to do this, however) as depicted in Fig. 18. The duty cycle is 0.9 and the dc voltage is adjusted to 391 V, so that the fundamental component of the applied voltage is

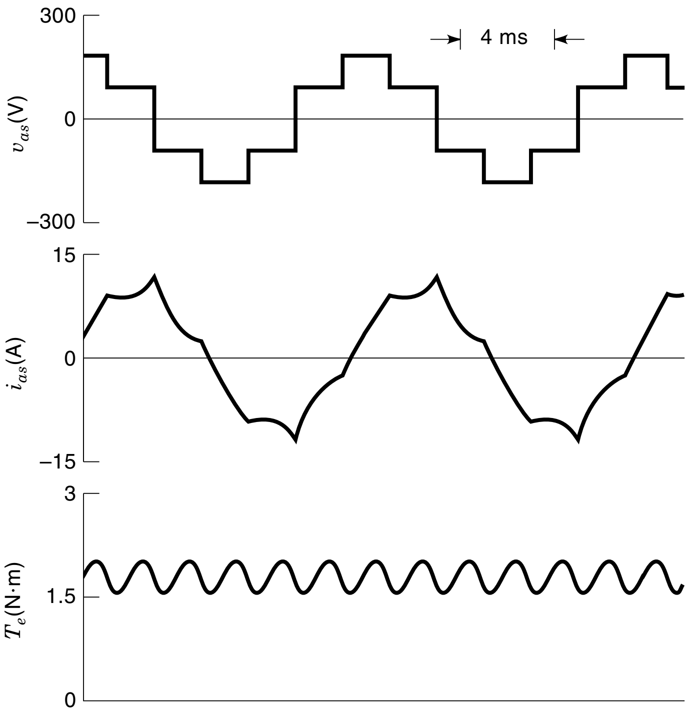


**Figure 17.** Operation of a 180° voltage-source, inverter-fed, permanent-magnet, synchronous machine. The voltage is a stepped approximation to a cosine waveform which results in undesirable low-frequency harmonics in the current and torque.

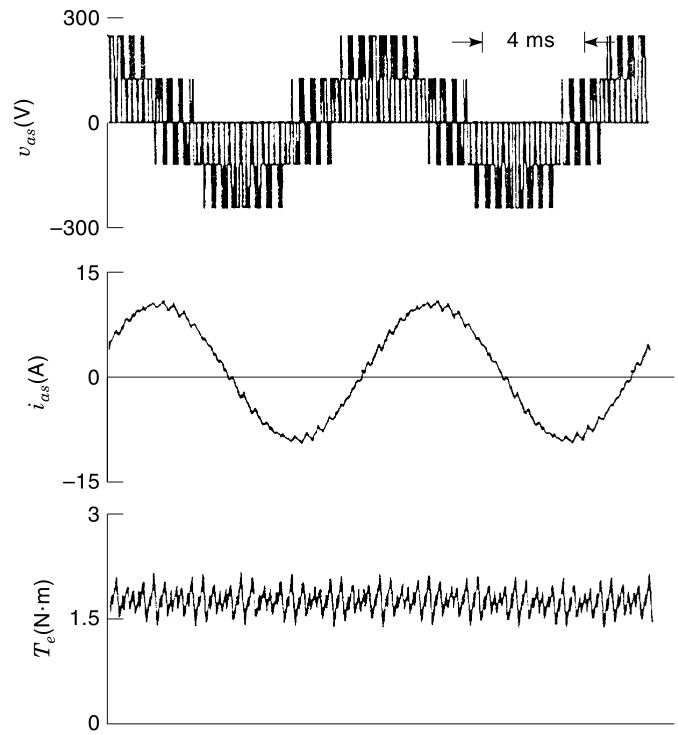


**Figure 18.** Operation of a sine-triangle modulated, voltage-source, inverted-fed permanent-magnet, synchronous machine. The voltage modulation improves the current and torque waveforms compared to the six-step operation shown in Fig. 17.

the same as in Fig. 17. In this case, the voltage, current, and torque waveforms contain high-frequency instead of low-frequency harmonics. This mode of operation is advantageous in terms of both current and torque ripple. Furthermore, the duty cycle is readily controlled to control the speed. Disadvantages of this control are the expense of the rotor position sensor and increased semiconductor switching losses.

Analyzing this type of drive system begins with determining the average-value of the applied $q$- and $d$-axis voltages. Transforming the fundamental component of the applied voltage to the rotor reference frame yields

$$\overline{v}_{qs} - mv_{dc}\cos(\phi_v) \tag{70}$$

and

$$\overline{v}_{ds} - mv_{dc}\sin(\phi_v) \tag{71}$$

where $m$ is a function of the modulation strategy used. In particular

$$m = \begin{cases} \dfrac{2}{\pi} & \text{for } 180^\circ \text{ operation} \\ \dfrac{2}{\pi}d & \text{for duty-cycle modulation} \\ \dfrac{1}{2}d & \text{for sine-triangular modulation} \end{cases} \tag{72}$$

**Table 1. Permanent-Magnet Synchronous Machine Parameters**

| | |
|---|---|
| $r_s$ = 2.985 Ω | $L_{ls}$ = 1.84 mH |
| $L_{mq}$ = 9.51 mH | $L_{md}$ = 9.51 mH |
| $P$ = 4 | $\lambda_m$ = 0.156 V·s |

The phase advance $\phi_v$ is physically determined in software (and considered an input) for continuous type of rotor position sensing. If Hall-effect devices are utilized, the phase advance is dictated by the physical position of the sensors. If the machine windings are connected in a delta configuration, Eqs. (70–71) must be modified by multiplying the voltages by $\sqrt{3}$ and adding $\pi/6$ to the cosine and sine terms. The fundamental component of the rms voltage is computed from Eq. (64) and Eqs. (70–71) by

$$v_s = \frac{1}{\sqrt{2}}mv_{dc} \tag{73}$$

The machine $q$- and $d$-axis currents are determined by averaging the machine voltage Eqs. (28–29) and solving for currents. This yields

$$\bar{i}_{qs} = \frac{1}{r_s^2 + \omega_r^2 L_q L_d}[r_s\overline{v}_{qs} - \omega_r L_d \overline{v}_{ds} - r_s\omega_r\lambda_m] \tag{74}$$

and

$$\bar{i}_{ds} = \frac{1}{r_s^2 + \omega_r^2 L_q L_d}[\omega_r L_q \overline{v}_{qs} + r_s\overline{v}_{ds} - \omega_r^2 L_q\lambda_m] \tag{75}$$

The average torque is calculated by averaging Eq. (31) which yields

$$\overline{T}_e = \frac{3}{2}\frac{P}{2}[\lambda_m \bar{i}_{qs} + (L_d - L_q)\bar{i}_{qs}\bar{i}_{ds}] \tag{76}$$

In obtaining Eq. (76), the average of the product of the $q$- and $d$-axis currents is approximated. Given the average machine

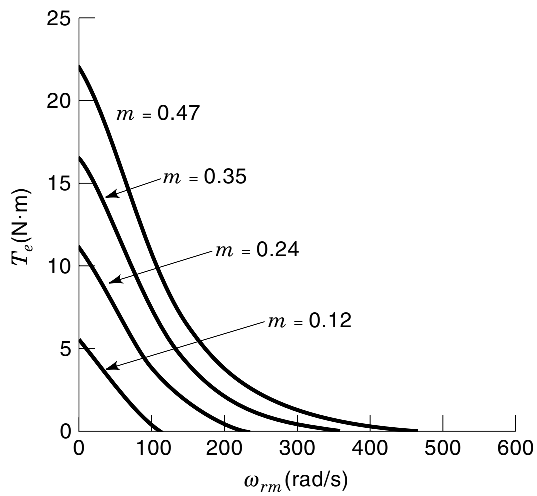


**Figure 19.** Torque vs speed characteristics of a voltage-source, inverter-fed, permanent-magnet, synchronous machine drive as the modulation index is varied. The applied voltage and, thus, the resulting torque increase with the modulation index.

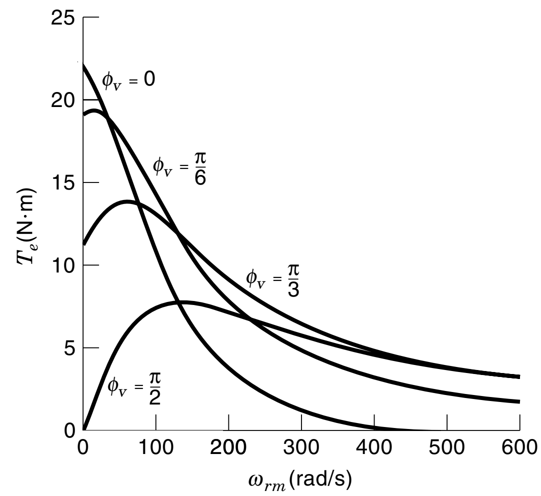


**Figure 21.** Torque vs speed characteristics of a voltage-source, inverter-fed, permanent-magnet synchronous machine drive as the phase advance is varied. The performance characteristics vary widely with the phase advance. A phase advance of zero provides the maximum stall torque whereas a phase advance of $\pi/2$ provides the maximum torque at high speeds.

voltages and currents, the remaining quantities of interest are readily determined by Eqs. (64–69).

Figures 19 and 20 illustrate average torque and the rms value of the fundamental component of the stator current versus rotor speed for several different values of the modulation index for the drive whose parameters are listed in Table 1. In this study, $v_{dc}$ is 300 V, and $\phi_v$ is zero. It can be seen that both torque and current decrease with speed, except that, after the torque passes through zero, the current begins to increase.

As it turns out, the phase advance has a pronounced effect on the torque-versus-speed characteristic of the synchronous motor drive. This is illustrated in Fig. 21 which depicts the torque-versus-speed of the drive with a dc voltage $v_{dc}$ of 300 V and a modulation index $m$ of 0.47 for several values of the phase advance. Setting the phase advance angle to zero provides the maximum stall torque (the torque at zero speed). A phase advance of $\pi/2$ provides the most torque at high speeds and zero torque at stall. Adjustment of the phase advance increases torque output at a given speed (1) or maximizes efficiency. In a system in which rotor position in sensed continuously, the phase advance may be varied with the operating point. When Hall-effect sensors are used however, the phase advance is fixed once it is selected. Optimizing for one operating point generally degrades the performance at other operating points.

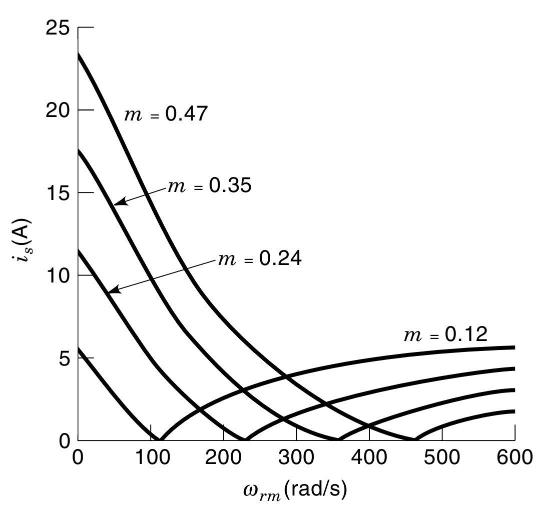


**Figure 20.** Rms current vs speed characteristics of a voltage-source, inverter-fed, permanent-magnet, synchronous machine drive as the modulation index is varied.

## CURRENT-REGULATED, INVERTER-FED, PERMANENT-MAGNET, SYNCHRONOUS MACHINE DRIVES

Another common configuration of synchronous motor drives is the current-regulated, permanent-magnet, synchronous machine drive which consists of a fully controlled, bridge converter connected to a permanent-magnet, synchronous machine with continuous rotor position feedback. In this case, the inverter is hysteresis modulated on the basis of $a$- $b$- and $c$-phase current commands, which are calculated in accordance with Fig. 22. (Note that current control is also possible with sine-triangle modulation using an inner current-control loop.) In the figure, based on torque command $T_e^*$ and speed $\omega_r$, the current command synthesizer determines the $q$- and $d$-axis current command ($i_{qs}^*$ and $i_{ds}^*$) so that the desired torque is obtained. In the case of a nonsalient machine, a simple current command synthesizer is given by

$$i_{qs}^* = \frac{T_e^*}{\frac{3}{2}\frac{P}{2}\lambda_m} \tag{77}$$

$$i_{ds}^* = 0 \tag{78}$$

In a nonsalient machine, this type of control maximizes efficiency because the $d$-axis current does not contribute to average torque. Occasionally, negative $d$-axis current is used to extend the speed range of the machine. In this case, the amount of $d$-axis current injected is a function of speed, torque, and dc voltage. Strategies for accomplishing this are set forth in (19,20) for salient and nonsalient machines, respectively. Once the $q$- and $d$-axis current command is established, the $abc$ variable current command $i^*_{abcs}$ is established using the inverse of Park's transformation given by Eq. (10).

One of the chief advantages of this drive system is that torque is controlled very rapidly and precisely. Figure 23 illustrates the performance of a current-regulated, permanent-magnet, synchronous motor drive during a step change in torque command. The machine parameters are identical to those used to produce Figs. 17 and 18, the dc bus voltage is 225 V, the hysteresis level is 0.6 A, and the current command synthesizer is given by Eqs. (77–78). In this study, machine is operating at a speed of 314.2 rad/s and a torque command of 1 Nm. Then the torque command is stepped to 2 Nm. Variables depicted include the torque command $T^*_e$, the $q$-axis current command $i^*_{qs}$, the $a$-phase current $i_{as}$, and the electromagnetic torque $T_e$. The $q$-axis current command is directly proportional to the torque command. Because of the high bandwidth of this type of control, the $a$-phase current and torque rapidly change to track the new reference during the step change in torque command.

To analyze current-regulated drives, for normal operating conditions, it is assumed that the actual $q$- and $d$-axis currents are equal to the commanded currents:

$$\bar{i}_{qs} = i^*_{qs} \tag{79}$$

and

$$\bar{i}_{ds} = i^*_{ds} \tag{80}$$

Then the average $q$- and $d$-axis stator voltages are expressed by the average of Eqs. (28–29) as

$$\bar{v}_{qs} = r_s\bar{i}_{qs} + \omega_r L_d \bar{i}_{ds} + \omega_r\lambda_m \tag{81}$$

and

$$\bar{v}_{ds} = r_s\bar{i}_{ds} - \omega_r L_q \bar{i}_{qs} \tag{82}$$

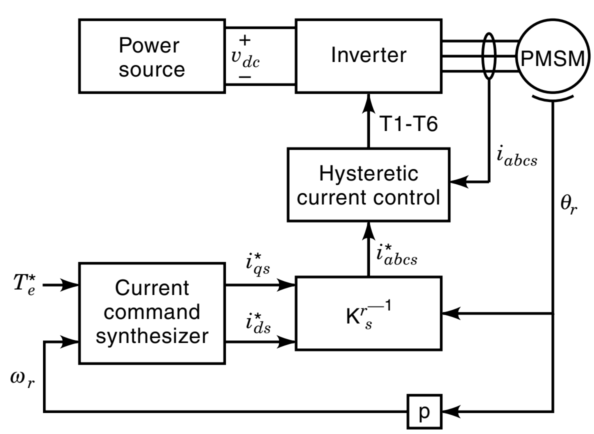


**Figure 22.** Current-regulated, inverter-fed, permanent-magnet motor drive configuration. The commanded current is generated by the current command synthesizer based on the commanded torque, machine speed, and machine parameters.

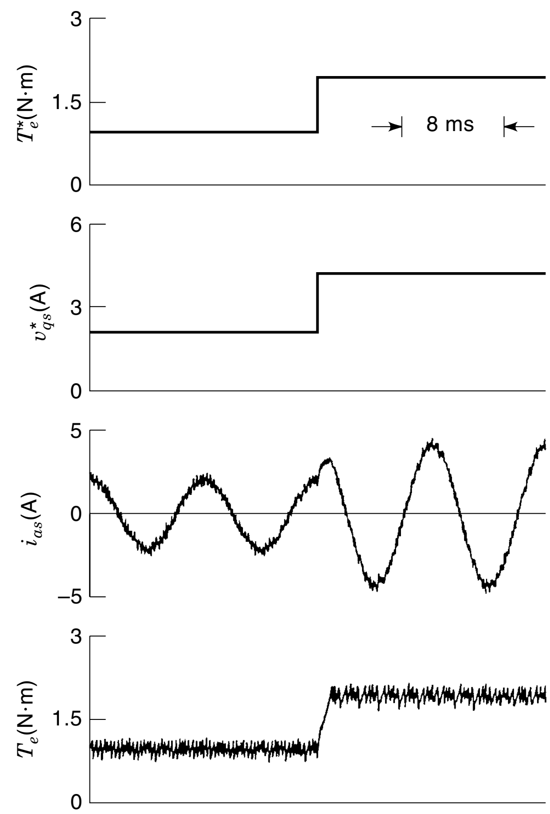


**Figure 23.** Operation of a hysteretic, current-regulated, inverter-fed, permanent-magnet, synchronous machine. For this type of machine, the $q$-axis current command is directly proportional to the torque command. When the current command is stepped up, the phase current increases. This increases the machine torque which closely tracks the commanded torque because of the high bandwidth of this type of control.

The machine torque is calculated from Eq. (76). Other quantities of interest are found from Eqs. (64–69).

Figure 24 illustrates the torque-versus-speed characteristics for several values of commanded torque. As can be seen for this type of drive system, torque is independent of speed in the low to mid speed range, as it must be if the actual currents are equal to the commanded current. As the speed increases, however, the actual currents no longer track the commanded currents. The condition for which this loss of tracking is expected to occur is given by Eq. (56). When analyzing the region where current tracking is lost, a much more involved analysis is required. The interested reader is referred to (18).

## VOLTAGE-SOURCE INVERTER-FED, SYNCHRONOUS-RELUCTANCE, MACHINE DRIVES

Although not as common as permanent-magnet, synchronous motor drives, synchronous-reluctance motor drives have advantages in terms of robustness (because there are no mechanically weak or temperature-sensitive permanent magnets). As with permanent-magnet motor drives, these devices are fed by voltage-source or current-regulated inverter modulating strategies. For voltage-source, inverter-based modulation, the same relationships for analyzing the voltage-source,

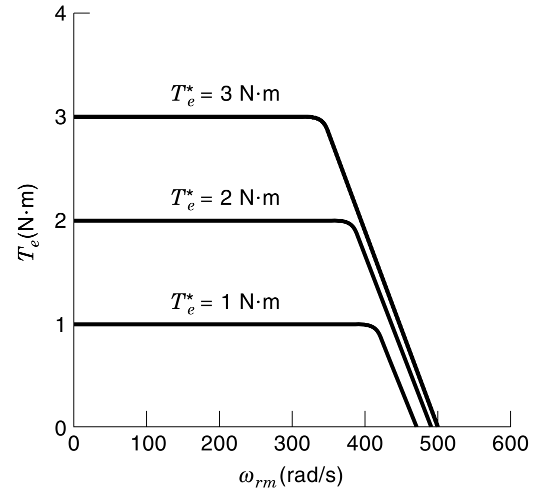


**Figure 24.** Torque vs speed characteristics of a hysteretic, current-regulated, permanent-magnet, synchronous machine drive as commanded torque is varied. Commanded torque is not achieved at high speeds because of the increased machine back-emf and the limited dc supply voltage.

inverter-based, permanent-magnetic, synchronous motor drives are used for the voltage-source, inverter-fed, reluctance motor drives except that $\lambda_m = 0$. Specifically, Eqs. (70–72) are used to calculate the motor average voltages, the average of Eqs. (74–75) are used to find the motor average currents, and Eq. (76) is used to find the average torque. Remaining quantities are readily determined from Eqs. (64–69).

Figure 25 depicts the torque versus speed curves, as predicted by the average-value model, of a voltage-source, inverter-driven synchronous-reluctance motor for several values of the phase advance angle. The motor parameters are given in Table 2. The dc voltage and modulation index for this study were 400 V and 0.48 respectively. As can be seen, the motor performance varies widely with the phase advance angle. At high speeds, a phase advance of $\pi/4$, which is equivalent to a delta angle of $-\pi/4$, produces maximum torque as is expected considering Eq. (8) or the reluctance torque curve of Fig. 3. At low speeds, however, the motor impedance is mostly resistive (nonreactive) and Eq. (8) is no longer valid. Setting the phase advance angle to $-\pi/4$ results in the maximum torque at stall. Values of phase advance between $-\pi/4$ and $\pi/4$ produce the intermediate performance curves shown in Fig. 25.

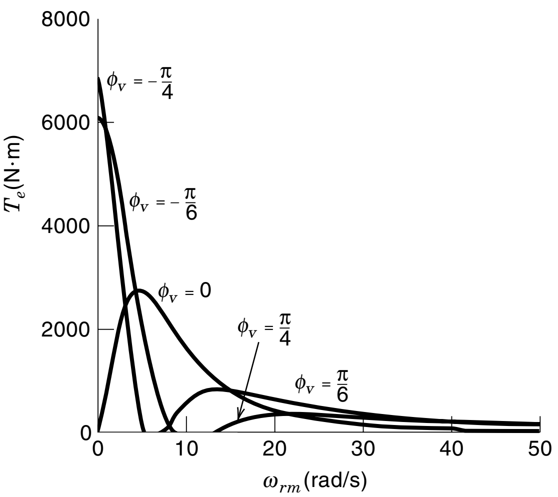


**Figure 25.** Torque vs speed characteristics of a voltage-source, inverter-fed, synchronous, reluctance machine drive as the phase advance is varied. The performance varies widely with the phase advance.

**Table 2. Reluctance Machine Parameters**

| | |
|---|---|
| $r_s = 0.382\ \Omega$ | $L_{ls} = 0.83$ mH |
| $L_{mq} = 13.5$ mH | $L_{md} = 39.27$ mH |
| $r'_{kq1} = 31.8$ mH | $L'_{lkq1} = 6.13$ mH |
| $r'_{kq2} = 0.923$ mH | $L'_{lkq2} = 3.4$ mH |
| $r'_{kd1} = 40.47$ mH | $r'_{lkd1} = 4.73$ mH |
| $r'_{kd2} = 1.31$ mH | $L'_{lkd2} = 3.68$ mH |
| $N_s/N_{fd} = 0.02711$ | $P = 4$ |

## CURRENT-REGULATED, INVERTER-FED, SYNCHRONOUS-RELUCTANCE, MACHINE DRIVES

Direct control of the machine currents offers the same advantage in the case of the synchronous-reluctance drive as it does in the case of permanent-magnet, synchronous machine drives, that is, rapid and precise control of the electromagnetic torque. As with the permanent-magnet motor drive, this is achieved by current regulation (such as hysteresis current control) or by having an inner control loop wherein voltage-source, inverter-based modulation is used to obtain voltages required to drive the actual currents to the desired currents. The analysis of this configuration is similar to that of the CRI permanent magnet motor drive with $\lambda_m = 0$, namely, Eqs. (77–78) are used to calculate the average $q$- and $d$-axis current, the machine voltages and torque are found from Eqs. (81–82) and Eq. (76), respectively. Other quantities of interest are readily obtained from Eqs. (64–69). As in the case of permanent-magnet synchronous machine drives with current-regulated inverter control, torque is easily and rapidly controlled, up to the point wherein the voltage capabilities of the inverter are insufficient to track the commanded currents.

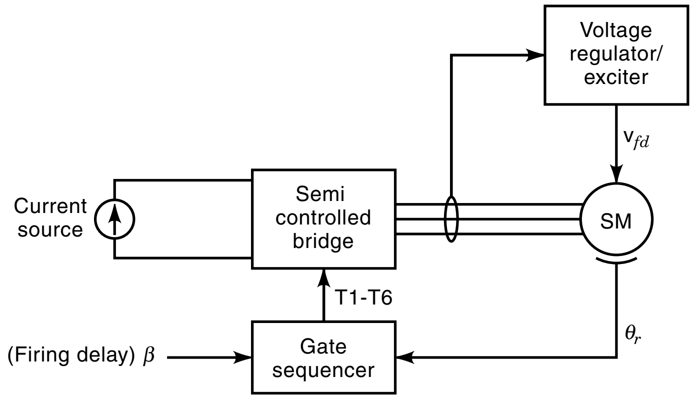


**Figure 26.** Synchronous motor drive using a semicontrolled three-phase bridge. The synchronous machine is supplied from a constant current source.

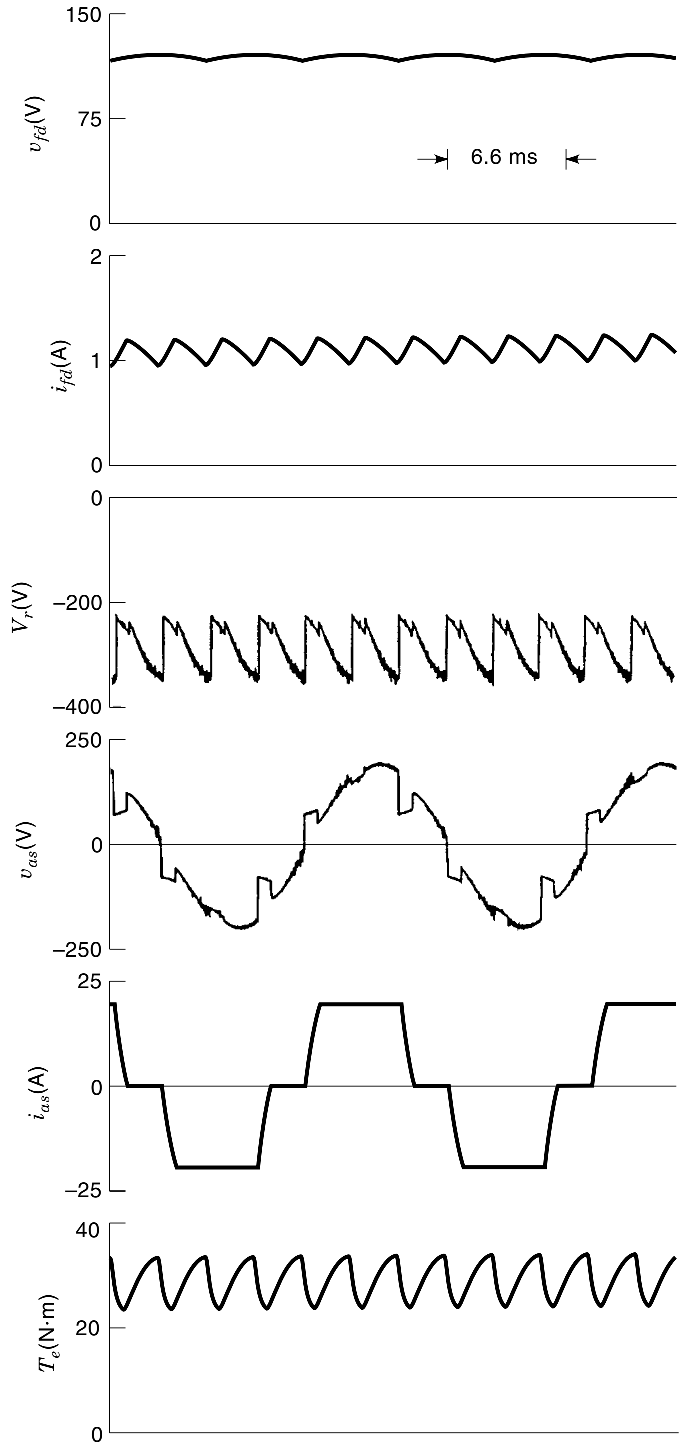


**Figure 27.** Operation of a wound-rotor, synchronous machine from a semicontrolled three-phase bridge. Positive torque and negative dc voltage indicate motor operation. Commutation is evident in the notches in the $a$-phase voltage.

## SEMICONTROLLED, INVERTER-FED, WOUND-ROTOR, SYNCHRONOUS MACHINE DRIVES

Because of the high voltage and current capabilities of thyristors, synchronous machine drives are often based on the semicontrolled rather than fully controlled bridge at high power levels. One possible configuration is illustrated in Figure 26 where a current source supplies a semi-controlled bridge (Fig. 13) which is, in turn, connected to a synchronous machine. This current source is synthesized by a voltage source coupled with an inductor and a closed-loop, current-control system. A voltage regulator/exciter monitors the terminal voltages of the machine and adjusts the field voltage of the synchronous machine so that the flux is at an appropriate level. To this end, a constant-volts-per-hertz scheme is employed. The firing of the inverter thyristors is based on rotor position. In this case, the gate sequencer operates as in Fig. 14 except that, instead of being fired relative to the back-emf, thyristors are fired from the rotor position. In particular, valve three is fired when

$$\theta_r = \frac{\pi}{3} + \beta \tag{83}$$

In Eq. (83), $\beta$ denotes the firing delay instead of $\alpha$ as in the previous discussion of semicontrolled converters because $\alpha$ is defined relative to the back-emf of the machine, not the rotor position. Firing relative to the rotor position is robust in that the firing sequence is unaffected by the harmonics in the terminal voltage induced by the rectifier. An alternate approach is to fire the converter based on the filtered terminal voltages.

Figure 27 depicts the performance of a 3.7 kW LCC synchronous machine drive whose parameters are listed in Table 3. In this study, the dc link current is regulated at 20 A, the terminal voltage is regulated at $v_s$ = 133 V, the electrical rotor speed is 377 rad/s, and the firing delay relative to the rotor position $\beta$ is 2.18 radians. Variables depicted include the field voltage $v_{fd}$, the field current $i_{fd}$, the rectifier voltage $v_r$, the $a$-phase line-to-neutral voltage $v_{as}$, the $a$-phase line current $i_{as}$, and the electromagnetic torque $T_e$. The small variation in the field voltage is the result of the harmonics in the line-to-line voltage, and the harmonics in the field current largely result from conservation of flux in the machine's $d$-axis. The notch in the rectifier and line-to-neutral voltages caused by commutation is clearly evident. As can be seen, the current waveforms are similar to the idealized waveform depicted in Fig. 14. The large amount of distortion in the current waveforms leads to considerable torque ripple, as depicted in the final trace.

Figure 28 depicts the average electromagnetic torque as $\beta$ is varied from 1.48 to 2.18 radians, as calculated from a computer simulation of a variety of operating points (the analytical solution is quite involved; the reader is referred to (12,21,22,23). The lower limit of $\beta$ is established by the approximate point where the average torque becomes positive, and the upper limit by commutation failure. Based on the pre-

**Table 3. Wound-Rotor Synchronous Machine Parameters**

| | |
|---|---|
| $r_s$ = 0.382 Ω | $L_{ls}$ = 0.83 mH |
| $L_{mq}$ = 13.5 mH | $L_{md}$ = 39.27 mH |
| $r'_{kq1}$ = 31.8 mH | $L'_{lkq1}$ = 6.13 mH |
| $r'_{kq2}$ = 0.923 mH | $L'_{lkq2}$ = 3.4 mH |
| $r'_{kd1}$ = 40.47 mH | $L'_{lkd1}$ = 4.73 mH |
| $r'_{kd2}$ = 1.31 mH | $L'_{lkd2}$ = 3.68 mH |
| $r'_{fd}$ = 0.122 mH | $L'_{lkd2}$ = 2.54 mH |
| $N_s/N_{fd}$ = 0.02711 | $P$ = 4 |

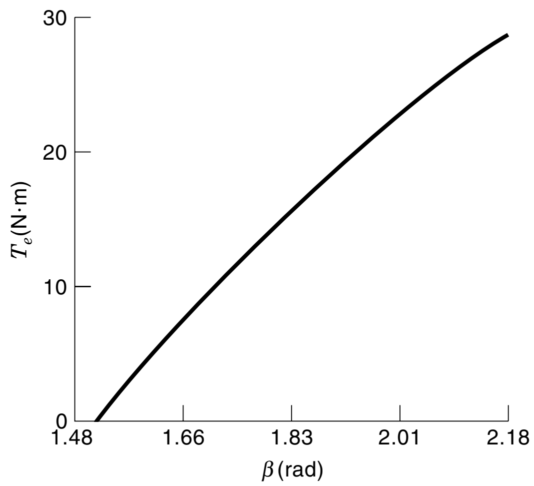


**Figure 28.** Torque vs $\beta$ of a semicontrolled, converter-fed, wound-rotor, synchronous machine drive. For maximum efficiency, it is desirable to operate with the largest value of $\beta$ possible. The upper limit of $\beta$ is determined by commutation failure.

vious discussion of firing delay, the reader may have suspected that the range over which the firing angle should be varied is approximately $\pi$ to $2\pi$ radians. The difference is caused by the fact that the firing angle controlled herein is the firing angle relative to the rotor position rather than the firing angle relative to the back-emf of the machine. As can be seen, it is desirable to operate with as large a firing delay as possible, while recognizing that, beyond a certain value, commutation failure occurs.

Besides commutation failure, another difficulty with this type of drive is start-up. In particular, at zero speed the machine does not possess a substantial back-emf necessary for the thyristor valves to commutate. Conditions and strategies for successful start-up are set forth in (24,25,26).

## BIBLIOGRAPHY

1. P. C. Krause, O. Wasynczuk, and S. D. Sudhoff, *Analysis of Electric Machinery,* Piscataway, NJ: IEEE Press, 1995.
2. R. H. Park, Two reaction theory of synchronous machines generalized method of analysis-part 1, *AIEE Trans.,* **48**: 716–727, 1929.
3. C. H. Thomas, Discussion of analogue computer representation of synchronous generators in voltage-regulation studies, *AIEE Trans.,* **75**: 1182–1184, 1956.
4. R. G. Harley, D. J. N. Limebeer, and E. Chirricozzi, Comparative study of saturation methods in synchronous machine models, *IEE Proc.,* **127, Part B** (1): 1–7, 1980.
5. K. A. Corzine, B. T. Kuhn, and S. D. Sudhoff, An improved method for incorporating magnetic saturation in the q-d synchronous machine model, Accepted for publication in *IEEE Trans. Energy Conversion,* 1997.
6. T. W. Nehl and N. A. Demerdash, Impact of winding inductances and other parameters on the design and performance of brushless dc motors, *IEEE Trans. Power Apparatus Syst.,* **104**: 2206–2213, 1985.
7. P. Pillay, Modeling of permanent magnetic motor drives, *IEEE Trans. Industrial Electron.,* **35**: 537–541, 1988.
8. R. R. Nucera, S. D. Sudhoff, and P. C. Krause, Computation of steady state performance of an electronically commutated motor, *IEEE Trans. Industrial Appl.,* **25**: 1110–1117, 1989.
9. S. D. Sudhoff and P. C. Krause, Operating modes of the brushless dc motor with a 120° inverter, *IEEE Trans. Energy Conversion,* **5**: 558–564, 1990.
10. S. D. Sudhoff and P. C. Krause, Average-value model of the brushless dc 120° inverter system, *IEEE Trans. Energy Conversion,* **5**, pp. 553–557, 1990.
11. H. W. Van Der Broeck, H. C. Skudelny, and G. V. Stanke, Analysis and realization of a pulsewidth modulator based on voltage space vectors, *IEEE Trans. Industry Appl.,* **24**: 142–150, 1988.
12. S. D. Sudhoff and O. Wasynczuk, Analysis and average-value modeling of line-commutated converter-synchronous machine systems, *IEEE Trans. Energy Conversion,* **8**: 92–98, 1993.
13. DC Motors, Speed Controls, Servo Systems: An Engineering Handbook, Eden Prairie, MN, Robbins & Myers/Electro-Craft, 1989.
14. D. C. Hanselman, Resolver signal requirements for high accuracy resolver-to-digital conversion, *IEEE Trans. Industrial Electron.,* **37**: 556–561, 1990.
15. T. Furuhashi, S. Sangwongwanich, and S. Okuma, A position-and-velocity sensorless control for brushless dc motors using an adaptive sliding mode observer, *IEEE Trans. Industrial Electron.,* **39**: 89–95, 1992.
16. N. Matsui and T. Takeshita, A novel starting method of sensorless salient-pole brushless motor, *Proceedings of the 1994 IAS Conference,* **1**: 386–392, 1984.
17. K. A. Corzine and S. D. Sudhoff, A hybrid observer for high performance brushless dc drives, *IEEE Trans. Energy Conversion,* **11**: 318–323, 1996.
18. K. A. Corzine, S. D. Sudhoff, and H. J. Hegner, Analysis of a current-regulated brushless dc drive, *IEEE Trans. Energy Conversion,* **10**: 438–445, 1995.
19. T. M. Jahns, Flux-weakening regime operation of an interior permanent-magnet synchronous motor drive, *IEEE Trans. Industry Appl.,* **23**: 997–1004, 1987.
20. S. D. Sudhoff, K. A. Corzine, and H. J. Hegner, A flux weakening strategy for current-regulated surface-mounted permanent-magnet machine drives, *IEEE Trans. Energy Conversion,* **10**: 446–454, 1995.
21. S. D. Sudhoff et al., Transient and dynamic average-value modeling of synchronous machine fed load commutated converters, *IEEE Trans. Energy Conversion,* **11**: 508–514, 1996.
22. S. D. Sudhoff, Analysis and average-value modeling of dual line-commutated converter-6-phase synchronous machine systems, *IEEE Trans. Energy Conversion,* **8**: 411–417, 1993.
23. S. D. Sudhoff, Waveform reconstruction from the average-value model of line-commutated converter-synchronous machine systems, *IEEE Trans. Energy Conversion,* **8**: 404–410, 1993.
24. T. Peterson and K. Frank, Starting of large synchronous motor using static frequency converter, *IEEE Trans. Power Apparatus Syst.,* **91**: 172–179, 1992.
25. R. L. Steigerwald and T. A. Lipo, Analysis of a novel forced-commutation starting scheme for a load-commutated synchronous motor drive, *IEEE Trans. Industry Appl.,* **15**: 14–24, 1979.
26. S. D. Sudhoff, E. L. Zivi, and T. D. Collins, Start up performance of load-commutated inverter fed synchronous machine drives, *IEEE Trans. Energy Conversion,* **10**: 268–274, 1995.

KEITH A. CORZINE
University of Wisconsin, Milwaukee
SCOTT D. SUDHOFF
Purdue University

**SYNCHRONOUS SYSTEMS CLOCK DISTRIBUTION.** See CLOCK DISTRIBUTION IN SYNCHRONOUS SYSTEMS.

**SYNCHROTRONS.** See SUPERCONDUCTING CYCLOTRONS AND COMPACT SYNCHROTRON LIGHT SOURCES.

**SYNTAX AND SEMANTICS.** See LOGIC PROGRAMMING AND LANGUAGES.

**SYNTHESIS OF NONLINEAR CIRCUITS.** See NONLINEAR CIRCUIT SYNTHESIS USING INTEGRATED CIRCUITS.

**SYNTHESIS (OR DESIGN) OF ANALOG PASSIVE FILTERS.** See FILTER SYNTHESIS.

**SYNTHESIS (OR DESIGN) OF LOSSLESS TWO-PORTS.** See FILTER SYNTHESIS.

**SYNTHESIS, HIGH LEVEL.** See HIGH LEVEL SYNTHESIS.

**SYNTHETIC APERTURE RADAR.** See REMOTE SENSING BY RADAR.